Southeast-Asian J. of Sciences: Vol. 2, No 1 (2013) pp. 63-70

SIMULATION OF ULTRASOUND IMAGE FROM CT-IMAGE DATA

Chau Huy Thong, Ly Anh Tu and **Pham Hoai An**

Department of Applied Physics, Faculty of Applied Science
University of Technology - VNU HCM
Ho Chi Minh City, Vietnam
e-mail: lyanhtu1@gmail.com; chthong89@gmail.com

Abstract

Real-time simulation of medical ultrasound imaging has an important role in clinic application. Quick access for training is highly concerned by improving technical skills to understand and process ultrasound image. In this paper, we describe the simulation of an ultrasound image with the presence of shadow effect that normally appears in real-time ultrasound imaging. We use the model of focused beam tracing in accompanying with tissue-ultrasound interactions, and apply CT scanning to obtain the map of scattering structure of imaging. The measured ultrasound image and CT image data are from database of Technical University of Denmark. FIELD II is then used to simulate an ultrasound image. It will be used for the purpose of synthesizing, analyzing and estimating the measured one and deducing an objective evaluation.

I. Introduction

Ultrasound (US) imaging in human body has been developed for over half a century[1] [2], and it is one of the most widely imaging method in medical diagnostic. The access to US data is limited due to data authorities, consequently it limits the research gateto discover a new US testing system. For simulation, we can use FIELD II program for US imaging simulation[3] [4]. It was implemented to use accompanying with Matlab for calculation and image processing, which helps us to optimize the image quality. Base on the software,

Key words: ultrasound imaging, Field II, CT image.

it is possible to design an appropriate number of various transducer geometries with multi-elements and various channels as well as beamformer methods for the simulation. We can modify and estimate the pulse-echo field, focusing schemes, scattering map, point spread function, and many useful parameters that influence our method of simulation based on the image point of view. Traditionally, US imaging in clinical diagnosis use the frequency range of several MHz to optimize the penetration and explore the superficial layer of an organ. For example, 2.5 MHz probe is used for a heart, 3.5 MHz for abdominal organs, and 7.5 or 10 MHz for surface layer explorations [5]. In this paper, we will evaluate the effect of high frequency range on fish body, to study how well we can estimate the consistency between US transducer model and acoustic properties of living organ using FIELD II.

II. Method of simulation

Field II program uses linear acoustic properties to calculate the transmitted and backscattered US fields as well as the pressure fields received at the transducer. For B-mode imaging, a number of independent scatterers are specified with their positions and amplitudes to simulate the scatterer maps of phantom models. A scatterer map can be derived from a CT image.

1. Theory of simulation

We can simplify the simulation model by considering rays which construct a sound beam. Suppose a ray has traveled from P_0 to P with initial intensity, and comes back along a reverse forward path to point P_0 passing through M media (M=5) as in Fig.1. A scatterer P is located inside a medium and the point source is at P_0. When the sound wave propagates through different media to the scatterer, only part of the sound energy is backscattered on the opposite path of the incident wave.

The attenuation of the incident intensity, I_I ,in two-way traveling from medium 1 to M and back is given by

$$I_{ATT} = I_I exp\big(-4\sum_{m=1}^{M} \alpha^{(m)} l_m\big) \tag{1}$$

where I_{ATT} is the attenuated intensity, $\alpha^(m)$ is the attenuation coefficient and l_m is the traveling distance of the sound wave in medium m^{th}. The intensity of transmission sound wave for two-way passing through m_{th} medium is given by [6]

$$I_{TR} = I_I \frac{4Z_m Z_{m+1} cos^2\theta_i^{(m)}}{(Z_m cos\theta_i^{(m)} + Z_{m+1} cos\theta_t^{(m)})^2} \tag{2}$$

where Z_m is the characteristic acoustic impedance of the m^{th} medium; θ_i

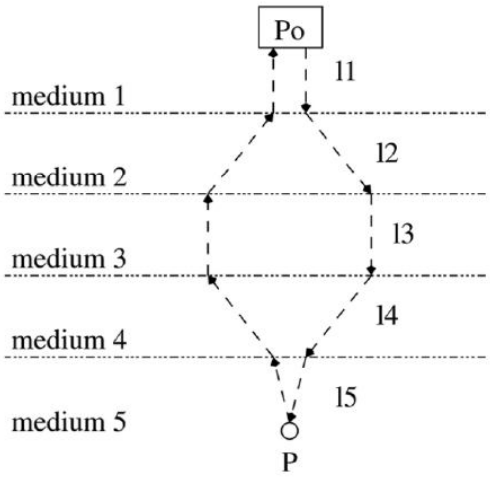

Figure 1: Ray tracing path [9]

and θ_t are the incidence and transmission angles between the surface normal and sound wave direction, respectively.

We assume that most of the intensity of the sound wave is scattered back to the transducer via reverse forward path, and the other rays that get back to P_0 in different paths are neglected. In the case the sound is transmitted to media as a ray perpendicular to the active aperture, the backscattered intensity I_{BS} is given by [7]

$$I_{BS} = I_I \frac{\eta_b^{(M)} V}{(\sum_{m=1}^{M} l_m)^2}, \tag{3}$$

where $\eta_b^{(M)}$ is the backscattering coefficient, and V is the volume of the scatterer.

Finally, with the assumption of no second- or higher-order harmonics scattering, very few scatterers on the boundaries between the media, and no loss of energy from the active aperture to the first medium corresponding to the top of the image. The received intensity at P_0 is [8] [9]

$$I_R(P) = I_I \frac{\eta_b^{(M)} V}{(\sum_{m=1}^{M} l_m)^2} exp(-4 \sum_{m=1}^{M} \alpha^{(m)} l_m) \times \prod_{m=1}^{M-1} \Big[\frac{4 Z_m Z_{m+1} cos^2 \theta_i^{(m)}}{(Z_m cos\theta_i^{(m)} + Z_{m+1} cos\theta_t^{(m)})^2} \Big]^2. \tag{4}$$

If a very small angle of incidence is assumed, $cos\theta = cos\theta_t \sim 1$, at all media

boundaries[9], we have

$$\frac{4Z_mZ_{m+1}cos^2\theta_i^{(m)}}{(Z_mcos\theta_i^{(m)}+Z_{m+1}cos\theta_t^{(m)})^2}\approx\frac{4Z_mZ_{m+1}}{(Z_m+Z_{m+1})^2}. \tag{5}$$

Therefore, we can simplify the formula for the final intensity calculation

$$\begin{aligned} I_R(P) &= I_I\frac{\eta_b^{(M)}V}{(\sum_{m=1}^{M}l_m)^2}exp\Big(-4\sum_{m=1}^{M}\alpha^{(m)}l_m\Big)\times\prod_{m=1}^{M-1}\left[\frac{4Z_mZ_{m+1}}{(Z_m+Z_{m+1})^2}\right]^2 \\ &= I_IV\times SSM(P) \end{aligned} \tag{6}$$

The final US scattering strength map, SSM(P), can be derived from formula (6) with the assumption that each pixel is a different medium, all scatterers within the medium have the same $l_{m'}$, and $I_IV=1$ (see [9]).

2. Scattering map from CT image

In the simulation, the values of attenuation coefficient, $\alpha^{(m)}$, backscattering coefficient, $\eta_b^{(M)}$, and acoustic impedance, Z_m , are calculated based on the CT image. Suppose that the tissue types of fish and human tissue types are pretty similar, we can segmented the CT image into four categories: bone, fat, soft tissue, air, and use the provided estimation in literature for these parameter values [6], [9]-[11].

Table 1: Coefficient from Hounsfield unit to backscatter, attenuation, and characteristic acoustic impedance [9]

Regions	Housfield unit	$\eta_b^{(M)}$(cm^{-1}sr^{-1})	$\alpha^{(m)}$(dB/cm MHz)	Z_m (kg/m^{2}s)
Bone	[179, maximum]	[0.05,0.1]	[100,200]	[6.5x10^6,7.38x10^6]
Soft tissue	[-41,178]	[0.000125,0.01]	[10,32.5]	[1.55x10^6,1.74x10
Fat	[-741,-42]	[0.003,0.019]	[1.25,2]	1.33x10^6
Air-inside	[minimum,-742]	0	[400,500]	0.4x10^3
Air-outside	Not defined by HU	0	0.24	1.48x10^6

Generally, the images of CT and US are scaled to the same size and orientation. Image boundaries were set close to the fish phantom where the number of scatterers is proportional to a cell resolution and an image volume. Scatterers are random uniform distribution in the tissue area, and multiplied with the Gauss distribution scatterer strength. Moreover, the HU values of outside area of the fish CT image are replaced by the HU values for water. A resolution of cell is calculated by [12]

$$ResCell = N\lambda FWHM_iFWHM_{azi}, \tag{7}$$

where λ is the wavelength and N is the number of cycles in the pulse; FWHM and FWHM$_{azi}$ are full width at half maximum laterally and azimuthally, respectively, of the point spread function at the focus point. The image volume

is calculated by multiplying CT image area with element height of transducer

$$imgVol = CTimage \times eleHeight. \tag{8}$$

The number of scatterers is then estimated with the recommended 10 scatterers per cell resolution[13]

$$n_{scatt} = 10 \times \frac{imgVol}{Rescell} \tag{9}$$

3. Simulation

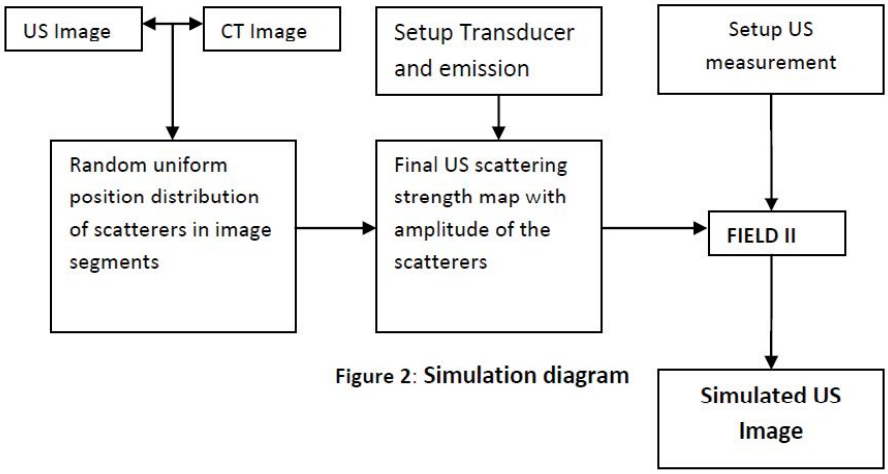

Figure 2: Simulation diagram

In the simulation, only some of the transducer elements are excited for each emission to produce an electronic focused US beam. The amplitudes of the scatterers were assigned which based on the final US scattering strength map using the position values. Corresponding to HU values of pixel in CT segments, the same scattering strengths were assigned for scatterers within particular medium. For the emission em_{th}, the US scattering strength for one emission,$SSM^{(em)}(P)$, is calculated by [9].

$$SSM^{(em)}(P) = \sum_{i=1}^{m} SSM_i^{(em)}(P), \tag{10}$$

where m is the number of active elements in one emission. $SSM_i^{(m)}(P)$ is calculated by Eq. (6) if the i^{th} ray passes through P. Otherwise, will be zero. For n emissions, the US scattering strength map is calculated by [9]

$$ASSM(P) = \frac{1}{n} \sum_{em=1}^{n} SSM^{(em)}(P). \tag{11}$$

The data of the measured CT and US image were obtained. The white line in Fig.3 indicates the CT slice with thickness of 0.5 mm and the pixel sizes 0.274 x 0.274 mm^2.

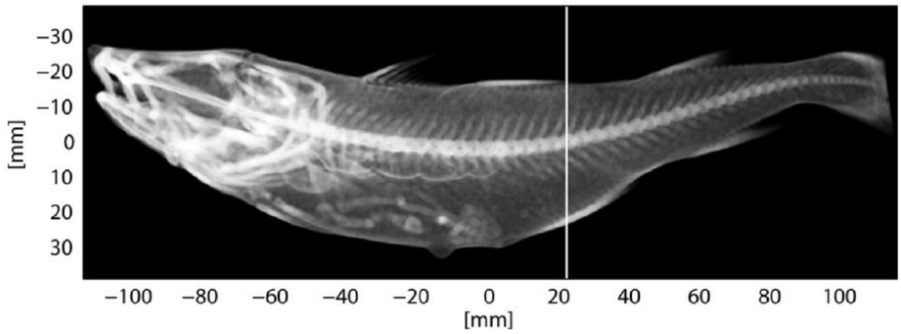

Figure 3: CT image of fish with a slice indication by a white line[9]

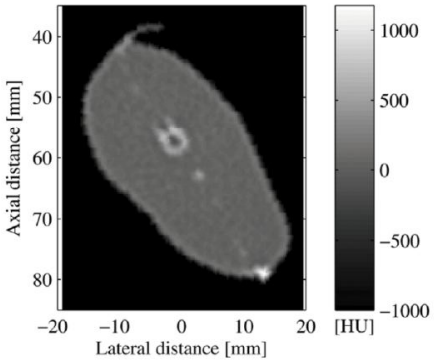

Figure 4: CT slice of fish[9]

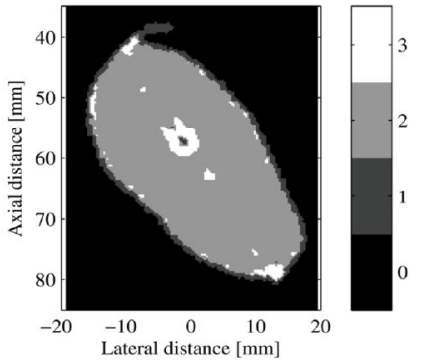

Figure 5: The region position map of the fish slice[9]

It is difficult to distinguish between fat and skin region in the CT image (Fig. 4) since they are next to each other, andhave very similar x-ray absorption. Therefore, the segment is then made manually to derive a region position map which represent in Fig. 5 (0: Air-outside, 1:Fat, 2: Soft tissue, 3: Bone.) The setup parameter was inputted to FIELD II, a transducer with 192 elements was used, the center frequency of transmit pulse was 10 MHz with 64 active elements; the transmit f-number was 3.65 and dynamic focusing was used with the receive f-number equal to 0.5. The process is to create 384 RF lines corresponding to 384 emissions in one US image. The number of scatterers is 10 per cell resolution. By modeling group of emission rays, the focus point is located at the center of the active aperture in the lateral direction and at the focus

depth of 45mm in the axial direction. The elevation focus is at 20mm depth. The number of rays is equal to the number of active elements.

3. Results and discussion

In the simulation, the slice thickness of the US imaging varies as a function of depth. It is narrowest, about 0.6mm, at the elevation focus of 20mm depth, and about 8mm at 80mm depth, while the effective slice thickness of the CT imaging modality is a constant, about 0.5mm. Hence, the simulation is more accurate at the elevation focus than at the other depths.

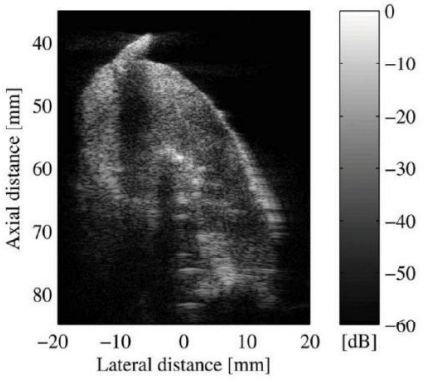

Figure 6: The measured US Image of the slice[9]

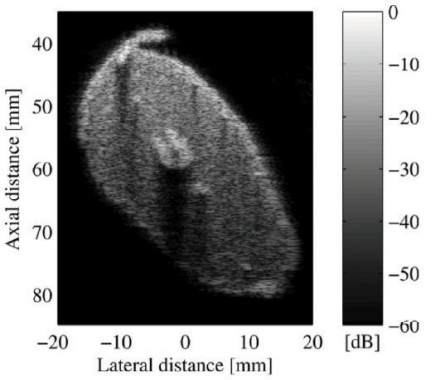

Figure 7: The simulated US image with shadow effect[9]

In the measured US image (Fig. 6), there are shadows appearing behind bone regions with high HU value and below the transition region, where sound passes through fish fin to water and gets into fish body. Similarly, the skin regions in the upper part of the fish get enhanced because the sound intensity decreases quickly in those regions. Most of these phenomena were included in the simulated US image (Fig. 7) except its uniformity looking like in CT image. The enhancement effect is only visible in the skin region on the upper part of the fish slice, where the high energy from the transducer is scattered back. The shadow effect was obtained with diffuse shape where the width of shadow is decreasing with depth.

IV. Conclusion

Even though the relation between Hounsfield Unit (HU) and US scattering strength is only local optimum with correct alignment of CT and US image in literature, this work has identified the potential to use CT image data to

show the consistency between fish US image with the simulation one. By using themethod of focused beam tracing model, the simulated US image has revealed most of the characteristics of measured US images such as shadowing, attenuation, and edge-enhancement. By using FIELD II, the transmitted and received apertures can be defined independently of each other. The acoustic settings can be controlled in the entire image through dynamic apodization and focusing. Frequency dependent attenuation can also be included in the simulation. The method is applied for a linear array transducer, but can be used for convex array and phase array transducers as well, because they also produce focused US beam in each emission. A similar mapping method could be used if the data are magnetic resonance, or optical images instead of CT-images.

References

[1] V. Chan and A. Perlas, *Basics of Ultrasound Imaging,* in Atlas of Ultrasound-Guided Procedures in Interventional Pain Management, S. N. Narouze, Springer, New York, 2011, pp. 1319.

[2] I. Edler and K. Lindstrm, *The history of echocardiography,* Ultrasound Med. Biol., **30**(12) (2004), pp. 15651644.

[3] J. A. Jensen, *FIELD: A Program for Simulating Ultrasound Systems,* in 10th Nordicbaltic Conference On Biomedical Imaging, **4**, Supplement 1, Part 1 (1996), pp. 351353.

[4] J. A. Jensen and N. B. Svendsen, *Calculation of pressure fields from arbitrarily shaped, apodized, and excited ultrasound transducers,* IEEE Trans. Ultrason. Ferroelectr. Freq. Control, **39**(2) (1992), pp. 262267.

[5] D. Lichtenstein, "General ultrasound in the critically ill", Springer, New York, 2005.

[6] J. A. Jensen, "Estimation of blood velocities using ultrasound: a signal processing approach, vol. Chapter 2., Cambridge University Press, 1996.

[7] R. W. Martin, *The interaction of ultrasound with tissue, approaches to tissue characterization and measurement accuracy,* in Practice of Clinical Echocardiography, C. M. Otto and A. S. Pearlman, editors., Philadelphia, W.B. Saunders Company, (1997), pp. 113129.

[8] M. Song, R. M. Haralick, and F. H. Sheehan, *Ultrasound imaging simulation and echocardiographic image synthesis,* in , Proceedings of 2000 International Conference on Image Processing, vol. **3**, pp. 420423.

[9] A. H. Pham, B. Lundgren, B. Stage, M. M. Pedersen, M. B. Nielsen, M. C. Hemmsen, and J. A. Jensen, *Shadow effects in simulated ultrasound images derived from computed tomography images using a focused beam tracing model,* J. Acoust. Soc. Am., **132** (2012) p. 487.

[10] J. C. Bamber, *Acoustical Characteristics of Biological Media,* in Encyclopedia of Acoustics, Icolm J. C. Editor-in-Chief, Ed. John Wiley & Sons, Inc., (2007), pp. 17031726.

[11] U. Schneider, E. Pedroni, and A. Lomax, *The calibration of CT Hounsfield units for radiotherapy treatment planning,* Phys. Med. Biol., **41**(1) (1996), pp. 111124.

[12] A. H. Pham, B. Stage, M. C. Hemmsen, B. Lundgren, and M. Mller, *Simulation of ultrasound backscatter images from fish,* in SPIE Medical Imaging, (2011), pp. 796152796152.

[13] T. A. Tuthill, R. H. Sperry, and K. J. Parker, *Deviations from Rayleigh statistics in ultrasonic speckle,* Ultrason. Imaging, **10**(2) (1988), pp. 8189.